60 In Positron Emission Tomography of the Brain - HEISS W. and PHELPS M. eds, Springer Verlag, 1983

A Method for Local Evaluation of the Volume of Rapidly Exchangeable Water in the Human Brain

By J. C. Depresseux

Introduction

The quest for optimal accuracy, precision, sensitivity, and spatial and temporal resolution of the measurements, combined with considerations of feasibility and noninvasiveness has led physiologists and biomathematicians to design many different methodological approaches to the determination of regional cerebral blood flow (rCBF) in man by means of externally detected radioactive inert indicators. Those methods are all based upon variants of the model initially designed by Kety and Schmidt (1948) to describe the kinetics of nitrous oxide in the whole brain.

One of the most cumbersome features of that group of techniques is the unavoidable introduction into the equations of a parameter – tissue-to-blood partition coefficient or distribution volume – characterizing tissular distribution of the indicator. Uncertainty about the regional value to be attributed to that parameter limits the accuracy of the results, especially when pathological cases are concerned.

The possibility of quantitative evaluation of tissular radioactive concentrations of indicators by positron emission tomography (PET) (Eichling et al. 1977; Hoffman et al. 1979; Huang et al. 1979a) enables the determination of the distribution volume of the tracers in CBF measurements (Yamamoto et al. 1979; Huang et al. 1981; 1982).

Among the numerous inert positron-emitting indicators used for evaluating rCBF (Ter-Pogossian et al. 1969; Jones et al. 1976; Subramanyam et al. 1978; Frackowiak et al. 1980; Yamatoto et al. 1979; Holden et al. 1981; Ginsberg et al. 1981), ^{15}O-labeled water has the advantages of diffusing rapidly across the blood-brain barrier (Raichle et al. 1976) and of being an important biological component whose distribution and kinetics are of utmost interest in themselves.

The purpose of the present investigation was the design, validation, and application of an original numerical method for the simultaneous determination of rCBF and the corresponding distribution volume of radiowater within the brain by bolus inhalation of $C^{15}O_2$ and sequential PET, with special attention paid to the possibility of evaluating the rapidly exchangeable water volume in the brain.

Material and Methods

The data for numerical analysis and for retrosimulation studies were obtained from normal subjects. Two modes of administration of $H_2{}^{15}O$ were sequentially used in five individuals: first, bolus inhalation from a bag of air mixed with 80 mCi $C^{15}O_2$, and second, after a delay of 20 min, continuous inhalation of 0.5 mCi/min $C^{15}O_2$ for 10 min.

Sequential PET detections of 53 s were performed from time zero of inhalation for 8 min with a whole body positron emission tomograph (ECAT II, EG & G ORTEC) (Phelps et al. 1978; Soussaline et al. 1979; Williams et al. 1979). Subjects remained in stable basal psychophysiological condition. Arterial blood gases were monitored. The tomographic plane was adjusted parallel to the orbitomeatal reference plane of the subject at a distance of 5 cm above it. Data were collected and reconstructed in the medium resolution mode (FWHM = 13.2 mm). The time course of radioactive concentration within the arterial blood was measured by catheterization of one humeral artery and by sequential counting of blood samples. Well counter and PET measurements were calibrated by imaging and counting radioactive concentrations in a pie phantom 20 cm in diameter.

Results and Discussion

General Equation of the Model

Whatever the method and time course of administration of the indicator, its concentration in each element of organ may be differentially described by the general equation:

$$dC_{bi}(t) = F_i C_a(t)dt - F_i C_{vi}(t)dt - \lambda C_{bi}(t)dt \quad (1)$$

with subscript i identifying the organ element under concern; t, the time; C_b, the radioactivity of radiowater within the organ element per unit mass of organ; C_a, the radioactivity of radiowater per unit volume of arterial blood; C_v, the radioactivity of radiowater per unit volume of venous blood; F, the blood flow perfusing the organ element in unit volume of blood per unit mass of organ and per unit time; λ, the radioactive decay constant of ^{15}O.

The variable $C_{vi}(t)$ is not accessible to measurement but may be expressed using the central volume theorem:

$$C_{vi}(t) = C_{bi}(t)/V_i \quad (2)$$

with V_i, the distribution volume of radiowater within the organ element i, expressed in unit volume per unit mass of organ (tissue + blood). Eqs. (1) and (2) classically give a general expression of the kinetics of the indicator through the element i of organ:

$$dC_{bi}(t) = F_i C_a(t)dt - (k_i + \lambda) C_{bi}(t)dt \quad (3)$$
with $k_i = F_i/V_i$

Solution from Data at Equilibrium

Most published research using $C^{15}O_2$ and $H_2{}^{15}O$ for the evaluation of rCBF utilizes continuous inhalation of $C^{15}O_2$ and PET detection performed at equilibrium of radioactive concentration of the indicator within blood and tissues (Ackerman et al. 1981; Lenzi et al. 1981; Bousser et al. 1980; Baron et al. 1978, 1981; Frackowiak et al. 1981).

The left member of equation (3) goes to zero at equilibrium, whereas $C_{bi}(t)$, $C_a(t)$ and $V_i(t)$ reach constant values. The CBF is then computed as:

$$F_i = \frac{\lambda}{C_a(equ)/C_{bi}(equ) - 1/V_i(equ)} \quad (4)$$

The accuracy, sensitivity and precision of this method were examined in recent papers (Jones et al. 1979, 1982; Huang et al. 1979b; Lammertsma et al. 1982). One of the limitations lies in the fact that the amount of data gathered at equilibrium is not sufficient for the evaluation of $V_i(equ)$, the value of which is presently derived from the normal total water content of brain tissue as measured by wet and dry weight differences. Any systematic error in $V_i(equ)$ is unfortunately propagated by Eq. (4) (Jones et al. 1982).

Solutions from Integrated Data from $t = 0$

The only way to gather sufficient information to evaluate F_i and V_i simultaneously is to collect data by rapid sequential PET after a bolus inhalation of $C^{15}O_2$ (Raichle et al. 1981; Huang et al. 1981, 1982) or during the equilibration phase occurring when the indicator is continuously inhaled.

Integration of Eq. (3) may be performed in two different ways.

The first possible solution uses *mathematical integration* (Huang et al. 1981) in the form of a convolution integral:

$$C_{bi}(t) = F_i \int_0^t e^{-(k_i+\lambda)(t-\tau)} \cdot C_a(\tau)d\tau \quad (5)$$

The numerical analysis giving F_i and V_i from observed data may be differently developed, depending on the expression which is given to the input function $C_a(t)$. For example, if $C_a(t)$ can be expressed as

$$C_a(t) = C_a(0)\, e^{-\mu t} \quad (6)$$

the formulae for computing F_i and V_i are as follows:

$$F_i = r_1 (k_i + \lambda) \quad (7)$$

$$V_i = F_i/k_i \quad (8)$$

with

$$k_i = \frac{\lambda + \mu - \lambda\mu r_2}{\mu r_2 - 1} \tag{9}$$

$$r_1 = \frac{\int_0^\infty C_{bi}(t)dt}{\int_0^\infty C_a(t)dt} \tag{10}$$

$$r_2 = \frac{\int_0^\infty tC_{bi}(t)dt}{\int_0^\infty C_{bi}(t)dt} \tag{11}$$

This approach suffers from the difficulty of necessarily (a) extrapolating of observed data up to $t = \infty$ and (b) fitting the observed input function with a suitable equation.

The second approach avoids convolution and uses *numerical integration* by integrating both members of Eq. (3):

$$C_{bi}(t) = F_i \int_0^t C_a(t)dt - (k_i + \lambda) \int_0^t C_{bi}(t)dt \tag{12}$$

Developments of Eq. (12) for data processing were recently published by Huang et al. (1982)

$$F_i = \frac{\lambda \int_0^T C^*_{bi}(t)dt - C_{bi}(T)}{\int_0^T C_a(t)dt \int_0^T C^*_{bi}(t)dt \int_0^T C_{bi}(t)dt - \int_0^T C^*_a(t)dt} \tag{13}$$

$$V_i = \frac{\lambda \int_0^T C^*_{bi}(t)dt - C_{bi}(T)}{\lambda \int_0^T C^*_a(t)dt - C_{bi}(T) \int_0^T C_a(t)dt / \int_0^T C_{bi}(t)dt} \tag{14}$$

with superscript * denoting radioactivities being time-corrected to time zero.

Contrary to the preceding method, this has the advantages of (a) using time integration of data from $t = 0$ to $t = T$ without necessitating any extrapolation and (b) integrating the input function by numerical procedure without mathematical fitting of data.

The model in use is exactly the same in both approaches but the latter fits actual data processing imperatives more easily.

Whatever procedure is chosen, it remains a prerequisite that the parameter V_i be submitted to very critical examination, taking into consideration (a) that it could be variable with time during the period of invasion of the organ by the indicator and (b) that it could not be equal to the tissue-blood partition coefficient of water as computed from brain and blood total content of water.

One of the objectives of the present investigation was to confront those two hypotheses with arguments derived from observed and simulated kinetics of radiowater within the brain tissue.

Stationariness of Volume V_i

The stationariness of the investigated volume V_i after bolus inhalation of $C^{15}O_2$ was tested by solving Eq. (3) in the form of the convolution integral (16): if the input function is generally described as

$$C_a(t) = C_a(0)\, e^{-\mu t} + A(t) \tag{15}$$

Eq. (3) may be solved:

$$C_{bi}(t) = \frac{C_a(0)F_i}{k_i + \lambda - \mu}\left(e^{-\mu t} - e^{-(k_i+\lambda)t}\right) + F_i\, e^{-(k_i+\lambda)t} * A(t) + \varepsilon_i(t) \tag{16}$$

with initial condition $C_{bi}(0) = 0$.

The parameter k_i in Eq. (16) is constant with time, with a resulting time-dependent error denoted $\varepsilon_i(t)$ if V_i is variable with time.

In all studied cases the arterial blood concentration measurements fitted the first term of Eq. (15) in the time interval ($1\ \text{min} \leqslant t < 10\ \text{min}$) with $r > 0.99$, μ being equal to the sum of the radioactive decay constant of ^{15}O and of the physiological decay parameter of the indicator concentration in the arterial blood. The difficult-to-fit function $A(t)$ vanishes for $t \geqslant 1$ min. Equation (16) is simplified and linearized as

$$\frac{C_{bi}(t)}{C_a(0)} = \frac{F_i}{k_i + \lambda - \mu}\left(e^{-\mu t} - e^{-(k_i+\lambda)t}\right) \tag{17}$$

and

$$Y_i(t, k_i) = \frac{F_i}{k_i + \lambda - \mu} X_i(t, k_i) \tag{18}$$

The parameter k_i in Eqs.(17) and (18) is then evaluated by iteration with search for best linear fitting. Figure 1 illustrates that it is possible to determine one value of k_i satisfying the linearity hypothesis of the relationship between observed values of $C_{bi}(t)$ and the modelized expression (17), for $t \geqslant 1$ min.

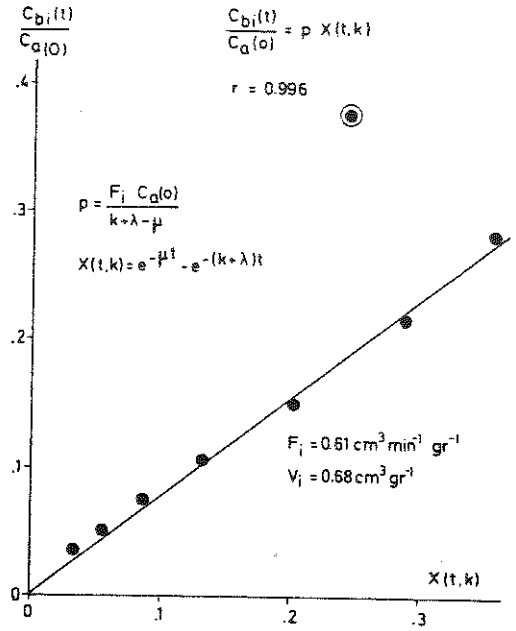

Fig. 1. Example of the linear relationship obtained by application of Eqs.(17) and (18) between observed and simulated values of $C_{bi}(t)$ in the time interval ($1\text{ min} \leqslant t < 8\text{ min}$): k_i was obtained by iteration and search for the best linear fit

Retrosimulation using Eq.(17) satisfyingly reproduced observed data within the same time interval in all cases (Fig. 2).

These convergent results validate Eq.(17) and the derived computing procedure. They allow furthermore the consideration that the second and third terms of the right member of Eq.(16) vanish for $t \geqslant 1$ min after a bolus inhalation of $C^{15}O_2$ and that V_i is therefore constant after that delay.

The bad mathematical prevision of $C_{bi}(t)$ by Eq.(17) for $t < 1$ min could result from the undefined input function $A(t)$ and from a possible initial variation in V_i, the incidence $\varepsilon_i(t)$ of which vanishes after 1 min.

In order to test the validity of the hypothesis of an initial variation of V_i, Eqs.(13) and (14) were successively applied to observed and simulated data.

Table 1 shows the bad convergence of computed values for V_i as obtained from observed data if increasing integration times are used in Eq.(14). As the input function is integrated by numerical procedure and thus fully determined from $t=0$, the bad convergence of results is suspected to be linked to a variation of V_i, the incidence of which is propagated in the results. The error propagation in Eqs.(13) and (14) due to an initial variation of V_i was studied by applying those equations to the analysis of simulated data obtained through Eq.(17) (Table 2). Both numerical procedures are in excellent correlation, provided that the whole transfer function $C_{bi}(t)$ is obtained from Eq.(17) from

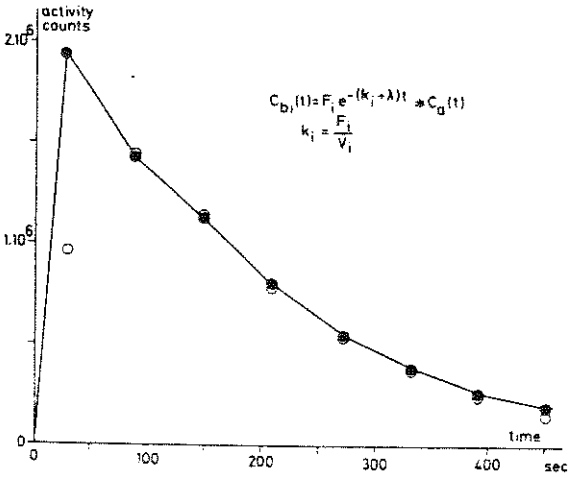

Fig. 2. Retrosimulation of $C_{bi}(t)$ using Eq.(17) and values of F_i and k_i obtained by iteration procedure. *Plain points*, observed data; *circles*, simulated values

$t=0$, i.e., that V_i is strictly constant. Slight fluctuations in the results are linked to approximations occurring within the numerical integration process.

In contrast, the introduction of a higher initial value of $C_{bi}(t)$, corresponding to a transitorily higher value of V_i, leads to an error which is propagated by Eqs. (13) and (14).

Comparison of results obtained from observed data, using both iteration and numerical integration procedures of analysis (Table 1), thus allows the inference that the discordance between observed and computed values of $C_{bi}(t)$ for $t<1$ min results not only from the difficulty in describing the early time course of $C_a(t)$

Table 1. Values of rCBF F_i and distribution volume of water V_i typically obtained from observed data with Eqs. (13) and (14), with increasing integration intervals from $t=0$ to $t=T$

T (s)	$C_{bi}(T)$ (ips/g)	F_i (cm^3/min per gram)	V_i (cm^3/g)
29.5	16145	−2.37	0.32
91.5	12960	−0.69	0.31
155.5	9290	−0.20	0.23
219.5	4549	0.06	−0.27
283.5	6251	0.15	6.70
347.5	2892	0.26	1.00
411.5	2179	0.26	1.03
475.5	1319	0.32	0.88

Table 2. Values of F_i and V_i obtained with Eqs. (13) and (14), with increasing integration intervals from $t=0$ to $t=T$. Data were obtained by simulation using Eq. (17). A disturbance introduced in the first value of $C_{bi}(t)$ is propagated by Eqs. (13) and (14)

T (s)	V_i constant in Eq. (17)			V_i initially variable [Eq. (16)]		
	$C_{bi}(T)$ (ips/g)	F_i (cm^3/min per gram)	V_i (cm^3/g)	$C_{bi}(T)$ (ips/g)	F_i (cm^3/min per gram)	V_i (cm^3/g)
26.5	15998	−5.04	0.20	32138	−10.12	0.39
86.5	22244	−2.78	0.26	22244	− 6.47	0.42
146.5	17895	−0.97	0.30	17895	− 2.11	0.42
205.5	12598	−0.18	0.22	12598	− 0.04	0.09
267.5	8261	0.19	1.48	8261	0.68	0.66
327.5	5377	0.37	0.69	5377	0.95	0.62
386.5	3493	0.46	0.64	3493	1.05	0.61
447.5	2226	0.51	0.61	2226	1.11	0.61

Table 3. Values obtained from observed data for F_i and V_i, using different numerical approaches: mathematical integration [Eqs. (7) to (11)], numerical integration [Eqs. (13) and (14)], and iteration procedure [Eqs. (17) and (18)]

Region	F_i (cm^3/min per gram)			V_i (cm^3/g)		
	Eq. (17)	Eq. (13)	Eq. (7)	Eq. (18)	Eq. (14)	Eq. (8)
1	0.57	0.57	1.09	0.59	0.68	0.69
2	0.68	0.70	1.90	0.67	0.79	0.76
3	0.70	0.98	3.47	0.63	0.71	0.70
4	0.70	0.79	2.47	0.69	0.78	0.74
5	0.69	0.84	1.61	0.56	0.62	0.67
6	0.84	0.91	3.13	0.52	0.57	0.58
7	0.60	0.57	1.20	0.59	0.69	0.69
8	0.56	0.62	1.58	0.72	0.81	0.76
9	0.69	0.90	2.25	0.64	0.70	0.74
10	0.48	0.55	1.36	0.70	0.76	0.71
11	0.71	0.79	2.11	0.57	0.64	0.64
12	0.68	0.66	1.68	0.52	0.59	0.59

mathematically, but also from an *initial variation of the distribution volume of radiowater.*
That variation of V_i during the period of invasion of brain tissue by radiowater could be considered as the result of an initial predominantly unidirectional extraction of the indicator, as was described in Crone's single-transit extraction model (1963).
The present investigation therefore invalidates classical solutions (5) and (12) of the differential Eq. (3), because the parameter V_i is time-dependant during the initial part of the integration interval.
The error resulting from that variation opportunely vanishes with time after the invasion period, with the possibility of a different approach to the data processing.
Results respectively obtained by mathematical integration [Eqs. (7) to (11)], by numerical integration [Eqs. (13) and (14)], and by iteration procedure are comparatively reported in Table 3.

Values of V_i with Different Input Functions

The stationariness of V_i for $t \geqslant 1$ min after bolus inhalation of $C^{15}O_2$ could lead to attributing the computed volume to a physically stable exchangeable water compartment. Additional arguments in favor of this hypothesis were derived by using a differently shaped input function of the indicator and by adapting the above iteration method.
Homologous values of F_i and V_i, obtained respectively from bolus (index B) and continuous (index C) inhalation of $C^{15}O_2$ are in good correlation, with a small systematical difference probably linked to the well-known difficulty of realizing a strictly constant rate of administration of the tracer with the continuous inhalation technique:

$$F_C = (0.101 + 0.787\ F_B)\ \text{cm}^3/\text{min g}$$
$$r = 0.942,\ n = 12$$
$$V_C = (-0.127 + 1.160\ V_B)\ \text{cm}^3/\text{g}$$
$$r = 0.948,\ n = 12$$

Figure 3 exemplifies values of F_i and V_i obtained in a normal subject in 5.3-cm^2 regions. The mean values of F_i and V_i in normal predominantly gray (index G) and white (index W) regions were (± 1 SD):

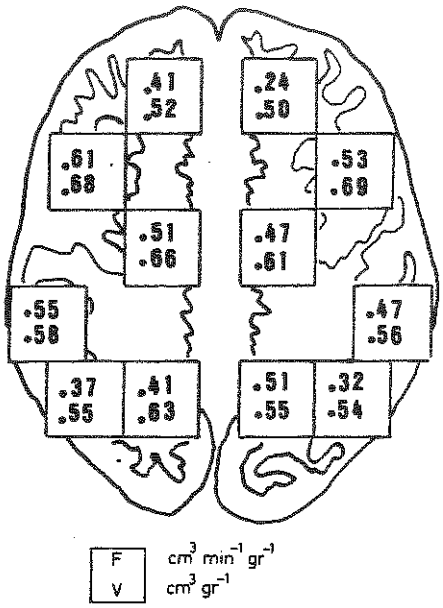

Fig. 3. Values of F_i and V_i obtained in a normal subject (plane 5 cm above the orbitomeatal line)

$$F_G = 72.7 \pm 8.0\ \text{cm}^3/\text{min 100 g}$$
$$F_W = 31.4 \pm 6.3\ \text{cm}^3/\text{min 100 g}$$
$$V_G = 69.6 \pm 5.4\ \text{cm}^3/100\ \text{g}$$
$$V_W = 59.3 \pm 5.0\ \text{cm}^3/100\ \text{g}$$

The volumes of rapidly exchangeable water in the brain matter which are derived by the present method are less than the total water content of gray and white matter (determined as around 0.85 cm^3/g in cortical gray matter and 0.71 cm^3/g in white matter (Torack et. al. 1976). The lower values of rapidly exchangeable water content as compared with total water content presumably correspond to the multicompartmental distribution of free and linked molecules of water within the cerebral tissue.

Conclusions

As previously stated (Huang et al. 1981, 1982), use of $H_2{}^{15}O$ and PET potentially allows non-invasive and quantitative evaluation of local cerebral blood flow and local distribution volume of radiowater within the human brain.
The present investigation, using detection and simulation data obtained with differently

shaped input functions of radiowater, provides arguments which allow us to infer that the cerebral distribution volume of radiowater does vary with time during the initial invasion period of tissue by the indicator and demonstrates that the observed variation leads to systemical errors and nonconvergence in results as long as the classical mathematical or numerical integration procedures are utilized for processing the data.

A different approach to the problem shows (a) that the regional distribution volumes of radiowater within the brain remain constant for 1–8 min after the bolus inhalation of $C^{15}O_2$ and (b) that the computed distribution volumes do not depend on the shape of the input function, be it a degradated delta function after bolus inhalation or a degradated square-wave function during continuous inhalation of $C^{15}O_2$.

Results argue for the validity of the model and its numerical expression and allow the so-determined distribution volume of radiowater to be considered as equal to a physiologically meaningful volume of rapidly exchangeable water of the brain tissue.

Applications of the method to clinical and pharmacological investigations are presently planned.

Acknowledgments. The author is grateful to J. P. Cheslet, J. Hodiaumont-Demblon, N. Walch, D. Lamotte, L. Quaglia, J. P. Peters, and G. Del Fiore for their respective contributions to his research. The work was supported by Grant 1.5.278.82 from the Belgian National Foundation for Scientific Research.

References

1. Ackerman RH, Correia JA, Alpert NM, Baron JC, Gouliamos A, Grotta JC, Brownell GL, Taveras JM (1981) Positron imaging in ischemic stroke disease using compounds labeled with 15-oxygen. Arch Neurol 38: 537–547
2. Baron JC, Comar D, Bousser MG, Soussaline F, Crouzel C, Plummer D, Kellershohn C (1978) Etude tomographique chez l'homme du débit sanguin et de la consommation d'oxygène du cerveau par inhalation continue d'oxygène-15. Rev Neurol 134: 545–556
3. Baron JC, Bousser MG, Comar D, Castaigne P (1981) Crossed cerebellar diaschisis in human supratentorial brain infarction. Trans. Am Neurol Assoc 105: 459–461
4. Bousser MG, Baron JC, Iba-Zizen MT, Comar D, Cabanis E, Castaigne P (1980) Migrainous cerebral infarction: a tomographic study of cerebral blood flow and oxygen-15 inhalation technique. Stroke 11: 145–148
5. Crone C (1963) The permeability of capillaries in various organs as determined by use of the "indicator diffusion" method. Acta Physiol Scand 58: 292–305
6. Eichling JO, Higgins CS, Ter-Pogossian MM (1977) Determination of radionuclide concentrations with positron C.T. scanning. (P.E.T.). J Nucl Med 18: 845–847
7. Frackowiack RSG, Lenzi GL, Jones T, Heather JD (1980) Quantitative measurement of regional cerebral blood flow and oxygen metabolism in man, using 150 and positron emission tomography: theory, procedure, and normal values. J Comput Assist Tomogr 4: 727–731
8. Frackowiak RSJ, Pozzilli C, Legg NJ, Du Boulay GH, Marshall J, Lenzi GL, Jones T (1981) Regional cerebral oxygen supply and utilization in dementia. A clinical and physiological study with oxygen-15 and positron tomography. Brain 104: 753–778
9. Ginsberg MD, Busto R, Lockwood AH, Finn RD, Campbell JA, Boothe TE (1981) 11C-Iodoantipyrine for the measurement of regional cerebral blood flow by positron emission tomography: synthesis and validation studies. J Cereb Blood Flow Metab 1 [Suppl. 1]: 37–38
10. Hoffman EJ, Huang SC, Phelps ME (1979) Quantitation in positron emission computed tomography: 1. Effect of object size. J Comput Assist Tomogr 3: 299–308
11. Holden JE, Gatlen SJ, Hichwa RD, Ip WR, Shaughnessy WJ, Nickles RJ, Polcyn RE (1981) Regional cerebral blood flow using positron emission tomography measurement of fluoromethane kinetics. J Cereb Blood Flow Metab 1 [Suppl 1]: 35–36
12. Huang SC, Hoffman EJ, Phelps ME, Kuhl DE (1979a) Quantitation in positron emission computed tomography: 2. Effects of inaccurate attenuation correction. J Comput Assist Tomogr 3: 804–814
13. Huang SC, Phelps ME, Hoffman EJ, Kuhl DE (1979b) A theoretical study of quantitative flow measurements with constant infusion of short-lived isotopes. Phys Med Biol 24: 1151–1161
14. Huang SC, Phelps ME, Carson R, Hoffman EJ, Plummer D, Mac Donald N, Kuhl D (1981) Tomographic measurements of local cerebral blood flow in man with 0-15 water. J Cereb Blood Flow Metab 1 [Suppl 1]: 31–32
15. Huang SC, Carson R, Phelps ME (1982) Measurement of local blood flow and distribution

volume with short-lived isotopes: a general input technique. J Cereb Blood Flow Metab 2: 99–108
16. Jones T, Chesler DA, Ter-Pogossian MM (1976) The continuous inhalation of oxygen-15 for assessing regional oxygen extraction in the brain of man. Br J Radiol 49: 339–343
17. Jones SC, Reivich M, Greenberg JH (1979) Error propagation in the determination of cerebral blood flow and oxygen metabolism with inhalation of $C15O_2$ and $15O_2$. Acta Physiol Scand 60 [Suppl 72]: 228–229
18. Jones SC, Greenberg JH, Reivich M (1982) Error analysis for the determination of cerebral blood flow with the continuous inhalation of 150-labeled carbon dioxide and positron emission tomography. J Comput Assist Tomogr 6: 116–124
19. Kety SS, Schmidt CF (1948) The nitrous oxide method for the quantitative determination of cerebral blood flow in man: theory, procedure and normal values. J Clin Invest 27: 476–483
20. Lammertsma AA, Heather JD, Jones T, Frackowiak RSJ, Lenzi GL (1982) A statistical study of the steady state technique for measuring regional cerebral blood flow and oxygen utilization using 15-O. J Comp Assist Tomogr 6: 566–573
21. Lenzi GL, Frackowiak RS, Jones T, Heather JD, Lammertsma AA, Rhodes CG, Pozzilli C (1981) $CMRO_2$ and CBF by the oxygen-15 inhalation techniques: results in normal volunteers and cerebrovascular patients. Eur Neurol 20: 285–290
22. Phelps ME, Hoffman EJ, Huang SC, Kuhl DE (1978) ECAT: a new computerized tomographic imaging system for positron-emitting radiopharmaceuticals. J Nucl Med 19: 645–647
23. Raichle ME, Eichling JO, Straatman MG, Welch MJ, Larson KB, Ter-Pogossian M (1976) Blood-brain barrier permeability of 11C-labeled alcohols and 150-labeled water. Am J Physiol 230: 543–552
24. Raichle ME, Markham J, Larson K, Grubb RL, Welch MJ (1981) Measurement of local cerebral blood flow in man with positron emission tomography. J Cereb Blood Flow Metab 1 [Suppl 1]: 19–20
25. Soussaline F, Todd-Pokropek AE, Plummer D, Comar D, Houle S, Kellershohn C (1979) The physical performances of a single slice positron tomographic system and preliminary results in a clinical environment. J Nucl Med 4: 237–249
26. Subramanyam N, Alpert NM, Hoop B, Brownell GL, Taveras JM (1978) A model for regional cerebral oxygen distribution during continuous inhalation of 15 O_2, C150 and $C15O_2$. J Nucl Med 19: 48–53
27. Ter-Pogossian MM, Eichling JO, Davis DO, Welch MJ, Metzger JM (1969) The determination of regional cerebral blood flow by means of water labeled with radioactive oxygen 15. Radiology 93: 31–40
28. Torack RM, Alcala H, Gado M (1976) Water, specific gravity and histology as determinants of diagnostic computerized Cranial Tomography (CCT). In: Pappius HM, Feindel W (eds) Dynamics of brain edema. Springer, Berlin Heidelberg New York, pp 129–137
29. Williams CW, Crabtree MC, Burgiss SG (1979) Design and performance characteristics of a positron emission computed axial tomograph – ECAT II. IEEE Trans Nucl Sc NS-26: 619–627
30. Yamamoto YL, Thompson C, Meyer E, Nukui H, Matsunaga M, Feindel W (1979) Three-dimensional tomographical regional cerebral blood flow in man measured with high efficiency mini-BGO two ring positron device using Krypton-77. Acta Neurol Scand 60 [Suppl 72]: 186–187